One-Step Synthesis of Polyaniline Nanofibers Decorated with Silver

Qingming Jia, Shaoyun Shan, Lihong Jiang, Yaming Wang

Faculty of Chemical Engineering, Kunming University of Science and Technology, Kunming 650224, China

Received 30 April 2008; accepted 27 August 2008
DOI 10.1002/app.30373
Published online 27 August 2009 in Wiley InterScience (www.interscience.wiley.com).

ABSTRACT: Polyaniline (PANI)/silver (Ag) nanocomposites containing PANI nanofibers decorated with well-dispersed Ag nanoparticles were obtained with interfacial polymerization. It was interesting that silver nitride affected not only the diameter and crystallinity of the PANI nanofibers but also their room-temperature conductivity. The conductivity increased with increasing Ag loading up to 10 (molar ratio of aniline to silver nitride), but the conductivity moderately decreased with further increasing Ag loading. Scanning electron microscopy and X-ray diffraction analysis results indicate that the diameter of the PANI nanofibers became smaller and smaller, and their crystallinity got better and better with increasing Ag loading. However, Fourier transform infrared analysis proved that the balance of oxidized and reduced units of PANI became big with increasing Ag loading, which may have resulted in the decreasing conductivity of PANI. © 2009 Wiley Periodicals, Inc. J Appl Polym Sci 115: 26–31, 2010

Key words: conjugated polymers; FT-IR; metal-polymer complexes; microstructure

INTRODUCTION

Because of their intriguing possibilities for structural modifications and promising potential applications in chemistry, biology, and materials sciences, organic–inorganic nanocomposites have received greater attention over the last few years. A wide range of organic and inorganic materials can be combined to form nanocomposites with unique electrical, catalytic, and optical properties.

Polyaniline (PANI) is a conducting polymer of particular interest because of its high stability, large conductivity range, low monomer cost, and the different redox states that can be obtained. More recently, PANI/metal composites have been extensively investigated for several reasons. First, these nanocomposites are expected to display several synergistic properties in applications such as catalysis,[1–4] sensors,[5–7] memory devices,[8,9] and fuel cells.[10,11] Second, the structures of PANI or metal can be well controlled by the interaction of PANI and metal salts. Third, the high surface-to-volume ratio of nanoparticles in these composites should result in a large number of binding sites available for chemical sensing or catalysis.

PANI/metal nanocomposites have been obtained by different methods: polymerization of aniline on the already formed metal nanoparticles,[12] reduction of metal salts by the already formed PANI,[13,14] a photoredox mechanism,[15] high-energy radiation,[16] or electrochemical methods.[17,18] In the aforementioned studies, much more emphasis was focused on the structure and properties of the metal nanoparticles, and few efforts have been made to investigate the morphology and properties of PANI simultaneously generated with the metal nanoparticles. Moreover, when nanocomposite materials containing PANI and metal nanoparticles are prepared, one major problem is that irregular granular PANI is obtained.

To solve this problem, we herein prepared PANI nanofibers decorated with well-dispersed silver (Ag) nanoparticles using interfacial polymerization and reducing Ag ions in the presence of PANI nanofibers. Because interfacial polymerization is one effective method of suppressing the secondary growth leading to nanofibers,[19–21] the morphologies of PANI/Ag nanocomposites may be controlled by interfacial polymerization. The room conductivity of the obtained products was tested by a four-probe method. The morphology and structure of these nanocomposites were characterized with scanning electron microscopy (SEM), X-ray diffraction (XRD), and Fourier transform infrared (FTIR) spectroscopy.

EXPERIMENTAL

Synthesis of the PANI/Ag nanocomposites

All chemicals were analytical grade and were used as received. Typically, the interfacial reaction was

Correspondence to: Q. Jia (kmustqmjia@163.com).

TABLE I
Conductivities of Pure PANI and PANI/Ag Nanocomposites

	Sample				
	Pure PANI	Aniline/Ag(1)			
		50	10	5	1
Conductivity (S/cm)	0.13	0.87	1.56	1.30	1.14

performed in a 50-mL glass tube, and the preparation process was similar to that of Kaner et al.[20] Aniline (2.2 mmol) was dissolved in the organic phase (chloroform, 15 mL) and was put into the glass tube. Then, ammonium peroxydisulfate (0.55 mmol, used as the oxidant) and quantitative silver nitride were dissolved in 1.0*M* nitric acid (15 mL, used as the solvent and dopant) at room temperature ($\sim$ 25°C). Thus, the obtained solution was carefully transferred to the glass tube so that an interface between the two layers could be performed. The polymerization reaction was carried out on the interface under static conditions for 24 h at room temperature. The resulting PANI/Ag composites were filtered and washed with deionized water and ethanol several times. Pure dark green powders were obtained after drying at room temperature for 24 h. In all reactions, the molar ratio of aniline to ammonium peroxyldisufate was kept at 4 : 1. The silver nitride content was varied from 0.0 to 2.2 mmol to investigate its effects on the structural and conductive properties of PANI.

Characterization

The morphologies of the resultant PANI/Ag were characterized with a field-emission scanning electron microscope (Philips XL 30 ESEM, Philips-FEI Co., Netherlands). Before SEM imaging, the samples were not sputtered with thin layers of gold. The molecular structures of PANI were measured by spectroscopy (IR Prestige-21, Shimadzu Co., Japan) and XRD (D/Max 2400, Rigaku Co., Japan). The electrical conductivity was determined by a standard four-probe method on PANI/Ag powders, which had been compressed into pellets 13 mm in diameter and approximately 0.5 mm in thickness with a SDY4 serial four-probe instrument (Guangzhou Four-Probe Technology Co., China).

RESULTS AND DISCUSSION

Conductivity test

The conductivities of the PANI/Ag nanocomposites with different Ag loadings are reported in Table I. The conductivity increased with increasing Ag loading up to 10 (molar ratio of aniline to silver nitride), in accordance with previous reports of PANI/metal nanoparticle composites.[22–24] When the molar ratio of aniline to silver nitride was 10, the conductivity of PANI/Ag was 12 times higher than that of pure PANI. However, the conductivity decreased with further increasing Ag loading.

XRD analysis

Figure 1 shows XRD spectra of the pure PANI and PANI/Ag with different Ag loadings. As shown in Figure 1, the XRD spectra of the PANI/Ag nanocomposites showed that these diffraction features appeared at about 38.1, 44.1, 64.4, and 77.3°, corresponding to the (111), (200), (220), and (311) planes of the cubic phase of Ag, respectively.[25] The size of the Ag particles (*D*) was determined with Scherrer's equation:[26]

$$D = \frac{0.89\lambda}{\beta \cos\theta} \tag{1}$$

where λ is the X-ray wavelength, β is the half-height width of the XRD peak, and θ is the Bragg angle. According to the β values of the Ag(111) and Ag(220) peaks, calculated with eq. (1), the Ag particle size in PANI/Ag (the molar ratio of aniline to silver nitride was 5 : 1) was calculated to be about 50 nm. The result means that the Ag in the PANI/Ag powder has a nanoparticle size. The letter "a" in

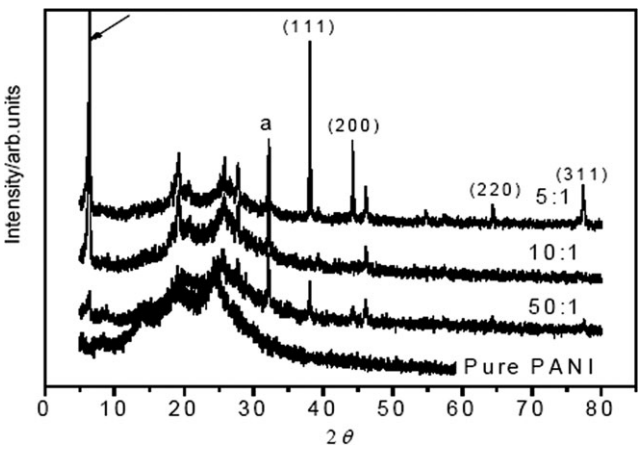

Figure 1 XRD spectra of pure PANI and PANI/Ag nanocomposites. The molar ratios of aniline to Ag(1) are shown.

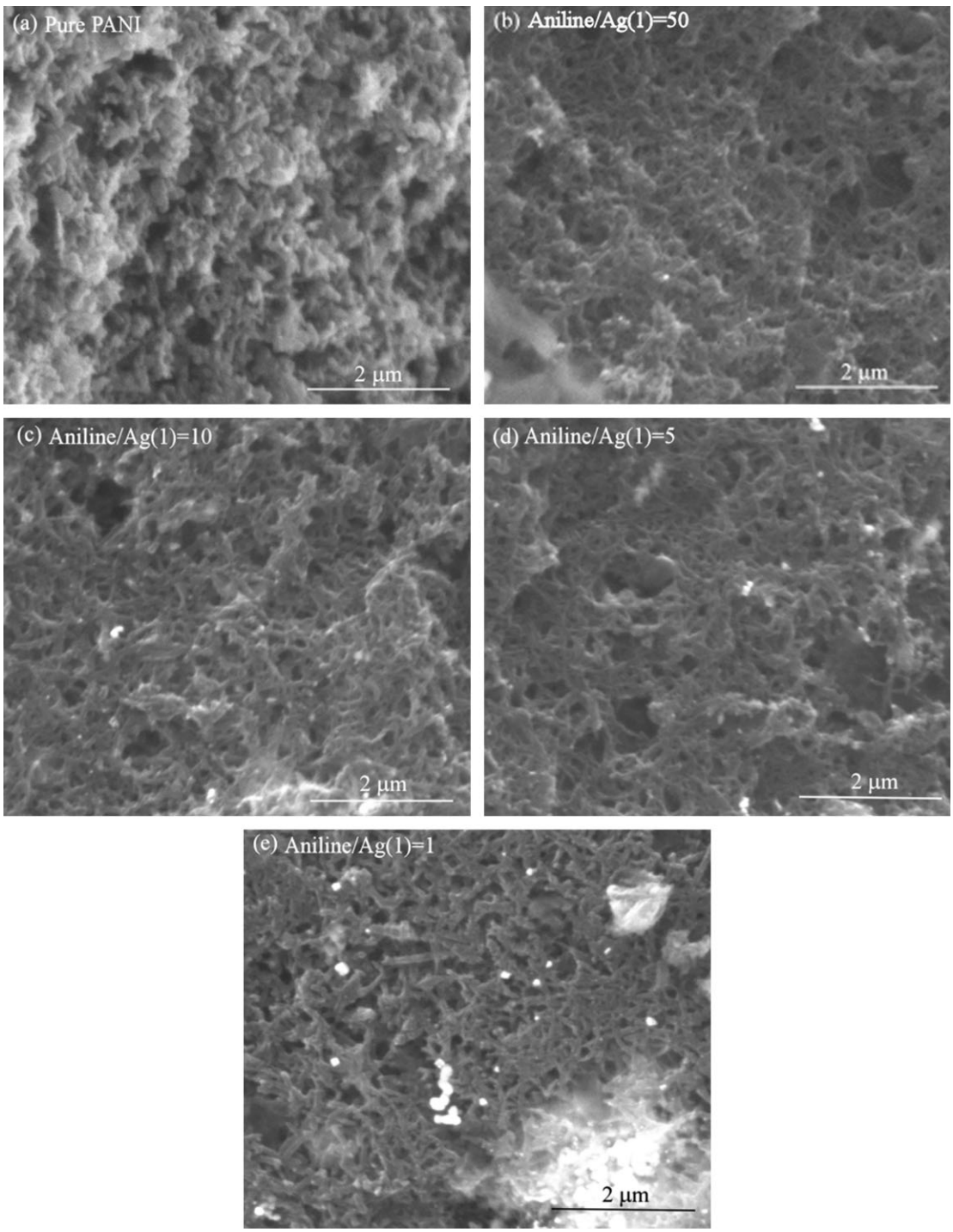

Figure 2 SEM images of pure PANI and PANI/Ag nanocomposites. The molar ratios of aniline to Ag(1) are shown.

Figure 1 designates diffraction peaks of the cube $Ag_2O(111)$.

Interestingly, significant differences in XRD between the PANI/Ag and pure PANI were also observed, as shown in Figure 1 (indicated a black arrow). As shown, a sharp peak at $2\theta = 6.34^\circ$, which was assigned to the periodic distance between the dopant and N atom on adjacent main chains, was observed for the PANI/Ag. Moreover, intensity of the peak became stronger and stronger with increasing Ag loading, which indicated the short-range order of the counterions along the polymer chain of the PANI/Ag. In addition, two broad bands centered at $2\theta = 19.7$ and 25.1°, which were ascribed to the periodicity parallel and perpendicular to the polymer chains of PANI, respectively, were observed in the pure PANI and PANI/Ag. However, the two bands became stronger and stronger

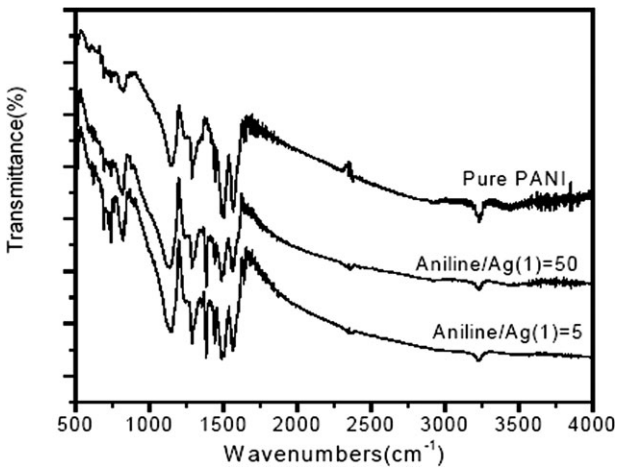

Figure 3 FTIR spectra of pure PANI and PANI/Ag nanocomposites. The molar ratios of aniline to Ag(1) are shown.

with increasing Ag loading. In particular, when the molar ratio of aniline to silver nitride was up to 5 : 1, there were two obvious bands at $2\theta = 19.7$ and 25.1°. These results show that the addition of Ag to PANI improved the crystallinity of PANI. The phenomenon could be explained by the following reasons. The polymerization rate was faster with increasing silver nitride content, and this was indirectly observed through the rapid color change of the reaction medium from transparent to blue. Because the fast polymerization shortened the growth time of PANI, the diameter of the PANI nanofibers became thin, and the crystallinity was high without undesired shapes. In addition to the catalytic effect of Ag(1) on the accelerating aniline polymerization, this phenomenon was attributed to the increasing number of available reaction sites on the polymer chain with decreasing Ag(1)/N molar ratio. The reduction of Ag(1) to Ag(0) is known to occur preferentially at the nitrogen groups of the PANI,[27] and a large number of sites can lead to a large number of smaller particles formed on these sites. This may also explain the trend shown for the higher Ag(1) concentration: a faster period of time was needed before the particles were large enough to be observed.

SEM analysis

The morphologies of the pure PANI and PANI/Ag are shown in Figure 2. Figure 2(a) indicates that the pure PANI consisted of nanofibers with diameters of around 50 nm, and the length of the fibers ranged from hundreds of nanometers to several micrometers. However, we observed that some aggregations existed in the pure PANI. When Ag(1) was added to the reaction system, the resultant PANI/Ag nanocomposites consisted of uniform nanofibers and spherical Ag nanoparticles, as shown in Figure 2(b–e). In addition, we observed that many fibers joined with others and formed branched structures or interconnected networks in the PANI/Ag nanocomposites. Comparing Figure 2(b) with Figure 2(c–e), one can see that the diameter of the PANI nanofibers decreased, whereas the diameter of the Ag nanoparticles increased with increasing Ag loading. The size of the Ag nanoparticles (bright regions) varied with changes in the aniline/metal salt ratio, typically when spherical Ag particles with diameters of around 20 nm formed at low Ag concentration (PANI/Ag = 50). These results reveal that the silver nitride concentration affected not only the morphology of PANI but also the size of the Ag nanoparticles.

FTIR analysis

Figure 3 shows the FTIR spectra of pure PANI and the PANI/Ag nanocomposites with different Ag loadings. Usually, the characteristic peaks at 1560–1580 and 1480–1500 cm^{-1} correspond to the C=C stretching of quinoid and benzenoid rings,[28] those at 1290–1305 and 1235–1245 cm^{-1} are related to the C—N and C=N stretching mode,[29] those at 1116–1145 cm^{-1} are assigned to the in-plane bending of C—H,[30] and those at 810–820 cm^{-1} are attributable to the out-of-plane bending of C—H.[31] The effect of Ag on the FTIR absorption of PANI is clearly shown in Figure 3. The characteristic peaks of pure PANI and the PANI/Ag nanocomposites with different Ag loadings are listed in Table II. As shown in Table II, a significant shift of the absorption peaks occurred when PANI was combined with Ag. The shifts of these absorption peaks were directly related to the differences in electron density. The shift to lower energy suggested that Ag, as the electron density donator, made the electron cloud of PANI more delocalized. A similar change in the FTIR absorption

TABLE II
Characteristic Peaks of Pure PANI and PANI/Ag Nanocomposites

Sample	$\nu_{quinoid\ ring\ stretch}$ (cm^{-1})	$\nu_{benzenoid\ ring\ stretch}$ (cm^{-1})	$\nu_{C-N\ stretching\ mode}$ (cm^{-1})	$\nu_{in-plane\ bending\ of\ C-H}$ (cm^{-1})	$\nu_{out-of-plane\ bending\ of\ C-H}$ (cm^{-1})
Pure PANI	1570.3	1500.2	1288.4	1151.5	821.7
Aniline/Ag(1) (50)	1566.2	1489.4	1243.1	1143.7	817.8
Aniline/Ag(1) (5)	1564.3	1487.1	1240.2	1145.7	817.8

TABLE III
***R* Values of Pure PANI and PANI/Ag Nanocomposites**

	Sample		
		Aniline/Ag(1)	
	Pure PANI	50	5
R	0.96	0.92	0.76

spectra of PANI was observed after combining with Au.[32]

The characteristic bands associated with the benzenoid phenyl ring (1500 cm^{-1}) and quinoid phenyl ring (1570 cm^{-1}) of the polymer were used to estimate the oxidation state of the polymer. The percentage of reduced units (x) versus the percentage of oxidized units (y) was obtained by integration of the FTIR bands:

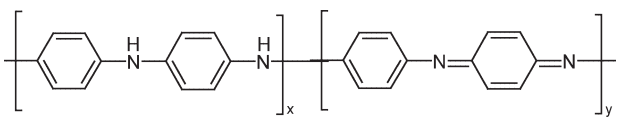

The ratio of x to y (R) for every sample is listed in Table III:

$$R = \frac{x}{y} = \frac{\text{Area}_{\text{reduced}}}{\text{Area}_{\text{oxidized}}} = \frac{\text{Area}_{\nu(1500\ \text{cm}^{-1})}}{\text{Area}_{\nu(1570\ \text{cm}^{-1})}} \quad (2)$$

where $\text{Area}_{\text{reduced}}$ is the oxidized units area, $\text{Area}_{\text{oxidized}}$ is the reduced units area, $\text{Area}_{\nu(1570\ \text{cm}^{-1})}$ is the area of ν(1570 cm^{-1}), and $\text{Area}_{\nu(1500\ \text{cm}^{-1})}$ is the area of ν(1500 cm^{-1}). As shown in Table III, pure PANI contained nearly identical percentages of oxidized and reduced units. However, R decreased with increasing Ag loading, which suggested that PANI's oxidized units increased, whereas the reduced units decreased. This was because the reduced units of PANI supplied protons to reduce Ag(1); each PANI repeating unit could convert two single charged metal ions into two metal atoms.[33] It is well known that the bigger the balance of oxidized and reduced units is, the lower the conductivity of PANI is. So the conductivity of the PANI/Ag nanocomposite slightly deceased when the molar ratio of aniline to silver nitride was 5, which was in accordance with the conductivity test.

CONCLUSIONS

In summary, PANI/Ag nanocomposites containing PANI nanofibers and well-dispersed Ag nanoparticles were obtained with interfacial polymerization. The conductivity increased with increasing Ag loading up to 10 (molar ratio of aniline to silver nitride). When the molar ratio of aniline to silver nitride was 10, the conductivity of PANI/Ag was about 12 times higher than that of pure PANI. However, the conductivity moderately decreased with further increasing Ag loading. SEM and XRD analysis results indicate that the morphology of the PANI nanofibers and their crystallinity changed with increasing Ag loading. FTIR analysis proved that the balance of oxidized and reduced units of PANI became big with increasing Ag loading, which may have resulted in a decrease in the conductivity of PANI. We believe that the synthesis approach presented in this article can be extended to other polymers/nanoparticles nanocomposites and should become a very effective route for controlling the morphology and properties of different nanocomposite materials. Efforts in this direction are currently being made in our laboratory.

References

1. Santhosh, P.; Gopalan, A.; Lee, K. P. J Catal 2006, 238, 177.
2. Amaya, T.; Saiom, D.; Hirao, T. Tetrahedron Lett 2007, 48, 2729.
3. Houdayer, A.; Schneider, R.; Billaud, D.; Ghanbaja, J.; Lambert, J. Appl Organomet Chem 2005, 19, 1239.
4. Park, J. E.; Park, S. G.; Koukitu, A.; Hatozaki, O.; Oyama, N. Synth Met 2004, 140, 121.
5. Wanekaya, A. K.; Chen, W.; Myung, N. V.; Mulchandani, A. Electroanalysis 2006, 18, 533.
6. Feng, X.; Mao, C.; Yang, G.; Hou, W.; Zhu, J. J. Langmuir 2006, 22, 4384.
7. Langer, J. J.; Filipiak, M.; Kecinska, J.; Jasnowska, J.; Wlodarczak, J.; Buladowski, B. Surf Sci 2004, 573, 140.
8. Tseng, R. J.; Baker, C. O.; Shedd, B.; Huang, J.; Kaner, R. B.; Ouyang, J.; Yang, Y. Appl Phys Lett 2007, 90, 053101.
9. Yang, Y.; Ouyang, J.; Ma, L.; Tseng, R. J. H.; Chu, C. W. Adv Funct Mater 2006, 16, 1001.
10. Chen, Z.; Xu, L.; Li, W.; Waje, M.; Yan, Y. Nanotechnology 2006, 17, 5254.
11. Lamy, C.; Belgsir, E. M.; Léger, J. M. J Appl Electrochem 2004, 31, 799.
12. Houdayer, A.; Schneider, R.; Billaud, D.; Ghanbaja, J.; Lambert, J. Synth Met 2005, 151, 165.
13. Smith, J. A.; Josowicz, M.; Janata, J. Phys Chem Chem Phys 2005, 7, 3614.
14. Smith, J. A.; Josowicz, M.; Janata, J. J Electrochem Soc 2003, 150, E384.
15. Khanna, P. K.; Singh, N.; Charan, S.; Viswanath, A. K. Mater Chem Phys 2005, 92, 214.
16. Lee, K. P.; Gopalan, A. I.; Santhosh, P.; Lee, S. H.; Nho, Y. C. Compos Sci Technol 2007, 67, 811.
17. Kinyanjui, J. M.; Hanks, J.; Hatchett, D. W.; Smith, A.; Josowicz, M. J Electrochem Soc 2004, 151, 113.
18. Kinyanjui, J. M.; Wijeratne, N. R.; Hanks, J.; Hatchett, D. W. Electrochim Acta 2006, 51, 2825.
19. Jia, Q. M.; Li, J. B.; Wang, L. F.; Zhu, J. W.; Zheng, M. S. Mater Sci Eng A 2007, 448, 356.
20. Huang, J. X.; Kaner, R. B. J Am Chem Soc 2003, 125, 126.
21. Huang, J. X.; Kaner, R. B. Angew Chem Int Ed 2004, 43, 5817.
22. Sarma, T. K.; Chattopadhyay, A. J Phys Chem A 2004, 108, 7837.
23. Sarma, T. K.; Chowdhury, D.; Paul, A.; Chattopadhyay, A. Chem Commun 2002, 21, 1048.

24. Pillalamarri, S. K.; Blum, F. D.; Tokuhiro, A. T.; Bertino, M. F. Chem Mater 2005, 17, 5941.
25. Sun, Y. G.; Yin, Y. D.; Mayers, B. T.; Herricks, T.; Xia, Y. N. Chem Mater 2002, 14, 4736.
26. Klong, H. P.; Alexander, L. E. X-Ray Diffraction Procedures for Crystalline and Amorphous Materials; Wiley: New York, 1954.
27. Neoh, K. G.; Tan, K. K.; Goh, P. L.; Huang, S. W.; Kang, E. T.; Tan, K. L. Polymer 1999, 40, 887.
28. Huang, K.; Wan, M. X. Chem Mater 2002, 14, 3486.
29. McCarthy, P. A.; Huang, J.; Yang, S. C.; Wang, H. L. Langmuir 2002, 18, 259.
30. Li, G. C.; Zhang, Z. K. Macromolecules 2004, 37, 2683.
31. Trakhtenberg, S.; Hangun-Balkir, Y.; Warner, J. C.; Bruno, F. F.; Kumar, J.; Nagarajan, R.; Samuelson, L. A. J Am Chem Soc 2005, 127, 9100.
32. Kinyanjui, J. M.; Hatchett, D. W.; Smith, J. A.; Josowicz, M. Chem Mater 2004, 16, 3390.
33. Li, W.; Jia, Q. X.; Wang, H. L. Polymer 2006, 47, 23.